Astronomy & Astrophysics

LETTER TO THE EDITOR

The secondary eclipse of the transiting exoplanet CoRoT-2b[*]

R. Alonso[1], T. Guillot[2], T. Mazeh[3,4], S. Aigrain[5], A. Alapini[5], P. Barge[6], A. Hatzes[7], and F. Pont[5]

[1] Observatoire de Genève, Université de Genève, 51 Ch. des Maillettes, 1290 Sauverny, Switzerland
e-mail: roi.alonso@unige.ch
[2] Observatoire de la Côte d'Azur, Laboratoire Cassiopée, CNRS UMR 6202, BP 4229, 06304 Nice Cedex 4, France
[3] Radcliffe Institute for Advanced Studies at Harvard, 8 Garden St. Cambridge MA 02138, USA
[4] School of Physics and Astronomy, R. and B. Sackler Faculty of Exact Sciences, Tel Aviv University, Tel Aviv 69978, Israel
[5] School of Physics, University of Exeter, Stocker Road, Exeter EX4 4QL, UK
[6] Laboratoire d'Astrophysique de Marseille, UMR 6110, Technopole de Marseille-Etoile, 13388 Marseille Cedex 13, France
[7] Thüringer Landessternwarte Tautenburg, Sternwarte 5, 07778 Tautenburg, Germany

ABSTRACT

We present a study of the light curve of the transiting exoplanet CoRoT-2b, aimed at detecting the secondary eclipse and measuring its depth. The data were obtained with the CoRoT satellite during its first run of more than 140 days. After filtering the low frequencies with a pre-whitening technique, we detect a 0.0060±0.0020% secondary eclipse centered on the orbital phase 0.494±0.006. Assuming a black-body emission of the planet, we estimate a surface brightness temperature of $T_{\rm p,CoRoT} = 1910^{+90}_{-100}$ K. We provide the planet's equilibrium temperature and re-distribution factors as a function of the unknown amount of reflected light. The upper limit for the geometric albedo is 0.12. The detected secondary is the shallowest ever found.

Key words. stars: planetary systems – techniques: photometric

1. Introduction

Out of the circa 350 exoplanets found to date, the 50 that transit their host stars allow several follow-up studies, based either on the occultation of part of the stellar disk by the planet (transits) or on the disappearance of the planet behind the star (secondary eclipses). Observations of the secondary eclipses of several exoplanets have enabled measurements of their emitted flux at different wavelengths, providing clues to their atmospheres (Charbonneau et al. 2005; Deming et al. 2005). Temperature inversions at stratospheric levels have been found on several occasions among the hottest known transiting Jupiters (Burrows et al. 2007; Knutson et al. 2008, 2009), and several detections of the modulation of the planetary flux with orbital phase have been claimed by Knutson et al. (2007) and Snellen et al. (2009).

The transiting planet CoRoT-2b (Alonso et al. 2008) was discovered during the first ~150-d pointing of the CoRoT mission (Baglin et al. 2006). The spectral type of the star (G0V) and the period of the planet (1.7 d) suggest that it belongs to the *pM* class of exoplanets as defined by Fortney et al. (2008), for which the strong incident flux is thought to cause stratospheric thermal inversions.

One of the intriguing characteristics of the hot Jupiters is their variety in planetary radius. While for several planets the measured radius agrees with theoretical models of planetary formation and evolution, some of them appear larger than expected.

A range of scenarios have been suggested to account for the phenomenon, but no clear picture has been delineated to date. CoRoT-2b not only belongs to this class of "bloated"' planets, but it is one with the most difficult radius as to explain, because of its high mass of $3.1 M_{\rm Jup}$.

The host star of CoRoT-2b exhibits several signs of youth (Bouchy et al. 2008), namely the detection of the Li I 6708 Å absorption line, an inversion of the cores of the Ca II *H* and *K* lines, and a faster-than-expected rotation period of 4.5 d (Lanza et al. 2009). While these "patterns" are traditionally attributed to stellar youth, it is also possible that the stellar evolution has been affected by tidal interactions with the close-in massive planet. Recently, Jackson et al. (2009) and Pont (2009) have suggested some observational evidence for strong tidal effects on exoplanets' host stars.

The activity of the star leaves footprints in the photometric light curve of CoRoT-2 that can be used to infer characteristics of the distribution and lifetimes of the spots on the stellar surface. By modeling the flux of the star in the parts of the light curve without transits, Lanza et al. (2009) observed a cyclic oscillation of the total spotted area of the star with a period of 28.9 ± 4.3 days. In a different study, Valio et al. (2009) looked at the effects of the occultation of spots in the planet's path along the stellar surface.

In this paper we describe detection of the secondary eclipse in the white light curve of the CoRoT public data. The technique is similar to the one used to detect the secondary eclipse of CoRoT-1b (Alonso et al. 2009b). A tentative detection of a 5.5×10^{-5} eclipse, based on the same data, has been claimed by Alonso et al. (2009a). Here we refine the analysis by carrying

---

[*] Based on observations obtained with CoRoT, a space project operated by the French Space Agency, CNES, with participation of the Science Program of ESA, ESTEC/RSSD, Austria, Belgium, Brazil, Germany, and Spain.

out a more careful filtering of the stellar variability, estimate the significance of the detection, and discuss the results.

2. Observations

CoRoT-2b was observed during the first *Long Run* pointing of the satellite, which lasted 142-days. We used the data corrected to the *N2* level (the processing steps are described in Auvergne et al. 2009), which contains 369 695 flux measurements, with a time sampling of 512-s from the first 5.2 days of data, after which it was changed to 32-s. The standard deviation of the normalized data after filtering the low frequencies as described below is 0.0014 (in units of normalized flux) for the 32-s sampled data, while it is 0.00056 for the 512 s data. For comparison, the photon noise level in the 32-s data is of 0.0011, revealing that the real data is only about 20% above the photon noise level, increasing to 90% above the photon noise in the 512-s part. An inspection of the 2MASS plates reveals that the star has a close companion 3.5 mag fainter in *V*, whose flux falls completely inside the aperture mask. We therefore subtracted a constant value of 5.6% of the median level of the curve before normalizing it, as in Alonso et al. (2008).

3. Analysis of the CoRoT light curve

The two most remarkable features of the light curve of CoRoT-2 are the transits by its companion and the modulation caused by the stellar activity and rotation. Both features tend to hide any secondary eclipse in the light curve; therefore, in this section we explain our efforts to filter these two features, while avoiding to dilute or erase the signal of the secondary eclipse.

To filter out the primary transit we could ignore the data points inside the transit. However, inclusion of data gaps at the orbital period of the transiting planet might result in spurious signals at this period and its harmonics, risking an effect on the signal of secondary eclipse. To reduce this risk, we subtracted the best fit solution of Alonso et al. (2008) from the curve, instead of cutting the parts of the light curves where the transits are detected. We plot the light curve with the transits removed this way in Fig. 1. As noted by Valio et al. (2009), the residuals in the individual transits show the effect of occulted spots during the transit, so they might add some high frequencies in a very short phase of the planet's orbit.

To filter out the stellar activity signal, we pre-whitened the light curve using PERIOD04 (Lenz & Breger 2005), a well-known and tested technique for identifying periodic signals in variable stars. Basically, it consists of successively locating the highest amplitude in the Fourier power spectrum and fitting a combination of sinusoids to the data that contain the frequency with the highest amplitude and all the previously identified frequencies. Before performing the PERIOD04 pre-whitening of the data, we averaged them into 30-min bins. We searched for frequencies between 0 and 24 c/d (cycles per day).
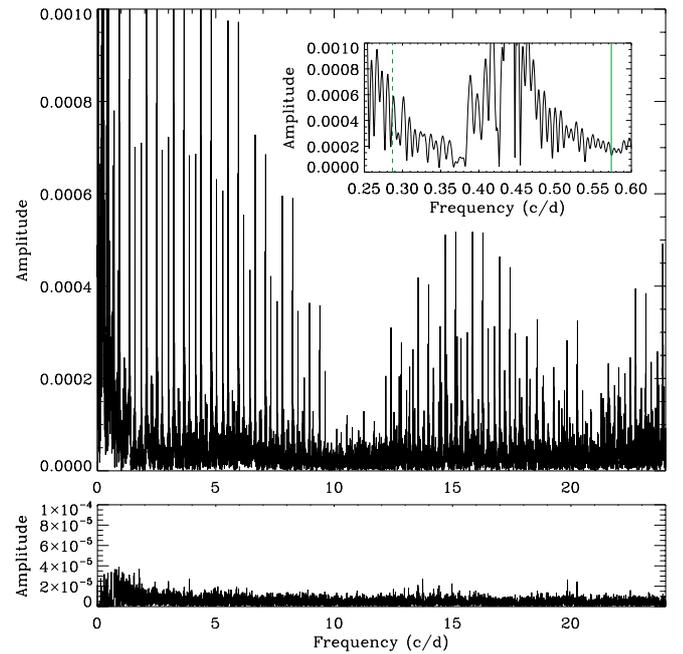
The amplitude spectra before and after filtering the low frequencies are plotted in Fig. 2, and the mean noise level in the 0-24 c/d range in the filtered spectum is of 6.1×10^{-6}, with a dispersion of 4.2×10^{-6}.

The search for the secondary eclipse was performed using the same techniques as described in Alonso et al. (2009b). Briefly, the search consisted of:

– selecting an orbital phase ϕ_i where the secondary depth is going to be evaluated;
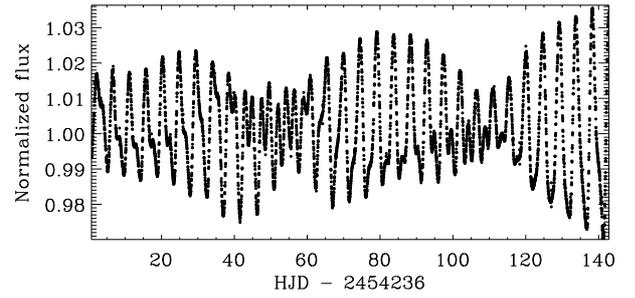
Fig. 1. Light curve of CoRoT-2 where the modeled transits have been subtracted. For display purposes, the data have been binned in 30 min bins.

Fig. 2. The amplitude spectra of the CoRoT-2 light curve, before (*top*) and after (*bottom*) pre-whitening of the 123 frequencies needed to model the low frequency content of the signal. To avoid including gaps in the data, the transits were previously corrected by the best-fit model of Alonso et al. (2009a). The inset shows a zoom around the planet's orbital frequencies. The vertical solid and dashed green lines mark the planet's period and twice that value, respectively.

– performing low order polynomial fits (linear fits in this particular case) to the parts of the light curve surrounding the phase ϕ_i. The regions where the fits are evaluated are at a distance of slightly more than the transit duration, to avoid including an hypothetical secondary centered on ϕ_i in the fits. The total number of fits will thus be the same as the total number of observed secondary eclipses;

– fitting a trapezoid with the same duration and shape as obtained from the transit parameters, and centered on ϕ_i. The only free parameter is the trapezoid depth.

The resulting plot of the significance and depth of a secondary eclipse as a function of the orbital phase is given in Fig. 3. The highest peak in this diagram appears close to phase 0.5, corresponding to a depth of about 6×10^{-5}.
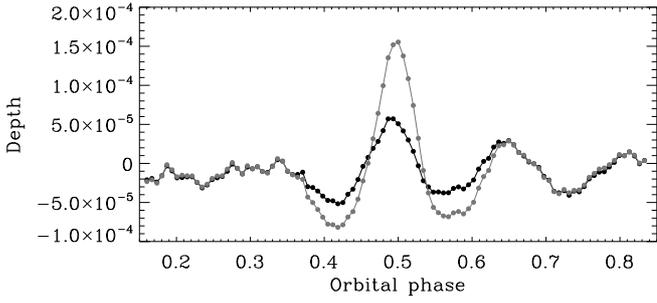
Fig. 3. Depth of a trapezoid with the shape and duration of a transit, as a function of the planet's orbital phase. The maximum is centered on phase 0.5, corresponding to the secondary eclipse. In gray, the result in a light curve where a secondary eclipse of 1×10^{-4} has been added to the raw light curve.

To make sure that any of the corrections explained above did not add or remove some signal of the secondary eclipse, we inserted a 0.01% secondary eclipse in phase 0.5 to the raw light curve, and performed the same analysis on this *simulated* data. The whole procedure, using the same filtering and repeating the pre-whitening of the curve, was performed on the *simulated* data. The results are plotted in Fig. 3, along with the results of the real data. The highest peak in this case is also centered at 0.5, and the fitted depth is of about 1.6×10^{-5}, i.e., the sum of the inserted eclipse and the signal present in the data. We thus suggest that the whole preparation of the curve before performing the secondary search does not significantly alter the signal we want to measure.

The phase-folded light curve during the phases of expected secondary eclipse is plotted in Fig. 4, together with the best fitted trapezoids. We explored the goodness-of-fit through χ^2 function around phase 0.5, in a grid of secondary eclipse centers and depths. The model used for the secondary was a trapezoid with duration and shape fixed to those of the transit. The observed secondary eclipse was binned into bins of 0.001 in phase (~2.5 min), and we estimated the error of each bin as the standard deviation of the measurements inside the bin divided by the square root of the number of points inside the bin. We plot the resulting χ^2 dependence and the formal sigma contours in Fig. 5. A secondary eclipse with a depth of 0.0060±0.0020% is detected in the CoRoT light curve at an orbital phase of 0.494 ± 0.006.

To estimate the significance of the secondary eclipse detection, we performed the following test, which preserved the presence of correlated noise in the data. From the data we subtracted the fitted secondary eclipse and shifted the residuals circularly, and then fitted a trapezoid with the phase and shape expected from the primary eclipse. Again, the only parameter was the secondary eclipse depth. All our 1000 trials resulted in depths less than 0.006%, the depth derived from the real data. The mean fitted depth was 0.0001 ± 0.0008%, consistent with zero. Additionally, we checked the uncertainties in the depth measurement by two different methods. In the first one, we reinserted the fitted secondary eclipse after the residual curves of the previous test were constructed and evaluated the fitted depths. We estimated the 1-σ uncertainty from the standard deviation of the depths that were fitted during this test. The result of this test gave a depth of 0.0059 ± 0.0008%. As a second method, we fitted two Gaussian functions to (1) the distributions of points inside total secondary eclipse and (2) a subset of the part outside secondary eclipse, with the same number of points as (1) and with a
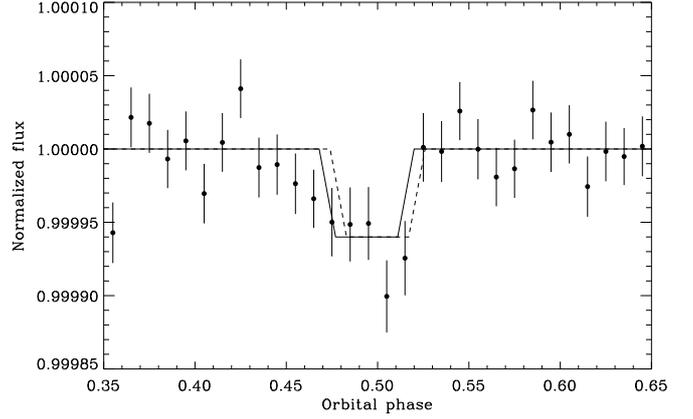
Fig. 4. Phase-folded curve of CoRoT-2b during the phases of secondary eclipse. The data have been binned in 0.01 in phase (~25 min), and the 1-σ error bars in each bin calculated as the standard deviation of the data points inside the bin divided by the square root of the number of points inside the bin. The solid line shows our best-fit trapezoid, with a depth of 0.0060 ± 0.0020%, and centered on phase 0.494 ± 0.006. The dashed line shows a secondary eclipse centered on phase 0.5.
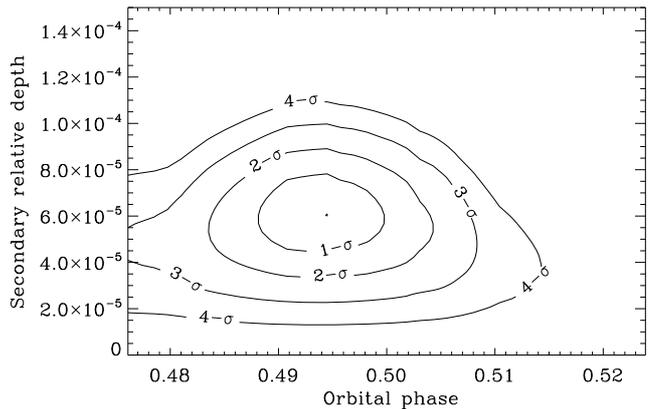
Fig. 5. The χ^2 value for different centers and depths of the secondary eclipse, and the 1, 2, 3, and 4-σ confidence limits.

randomly selected starting point. In the construction of the distributions, to minimize the effect of an arbitrarily selected histogram bin size, we used random values of the sizes of the histogram bin, between 1×10^{-6} and 7×10^{-6} in units of normalized flux. We repeated this test using 500 different starting points and values of the bin, and we estimated the 1-σ errors as above. This test resulted in a depth of 0.0066 ± 0.0020%. We adopted a final value of the secondary eclipse depth of 0.006 ± 0.002% from the results of the different tests.

The secondary eclipse appears slightly offset, at a 1-σ level, from the expected center for a circular orbit, which could be interpreted as a possible non-zero eccentricity of $e \cos \omega = 0.01 \pm 0.01$. This eccentricity is within the 1-σ uncertainty of the orbital solution obtained from the radial velocity measurements (0.03 ± 0.03 in Alonso et al. 2008).

4. Discussion

In the optical, the observed flux of the planet can be expressed:

$$F_p = F_{p,reflected} + F_{p,reemitted} + F_{p,internal}, \qquad (1)$$

i.e., the sum of a component of reflected light, a thermal re-emission of the incident stellar flux, and a thermal emission not related to the incident flux from the star (e.g., internal heat or emission due to tidal forces). The reflected light can be estimated as $F_{p,reflected} = A_g \left(\frac{R_p}{a}\right)^2$ where A_g is the geometric albedo. We can calculate the thermal component of the planet's emission (the combination of $F_{p,reemitted}$ and $F_{p,internal}$) using the same procedure as in Alonso et al. (2009b). For that purpose, we used a value of T_{eff} = 5625 ± 120 K for the star (Alonso et al. 2008) and the model spectrum of a G8V star from Pickles (1998). We calibrated the model spectrum to obtain the same integrated flux as a Planck function with the T_{eff} of the star. Taking the CoRoT spectral response function into account (Auvergne et al. 2009), the ratio of areas of the star and the planet, and the incident flux lost in the reflection ($A_B F_\star$ where A_B is the Bond albedo), we searched for the brightness temperature that matched the observed eclipse depth. We assumed a black-body emission for the planet and considered different values of the albedo. We assumed $A_B = A_g$, a reasonable assumption since more than 50% of the stellar flux is emitted at the CoRoT wavelengths. As an example, $A_B \sim A_g$ within 20% for the four solar system giant planets when integrating A_g between 0.4 and 0.9 μm (Karkoschka 1994). The different possible solutions are plotted in Fig. 6. The zero-albedo brightness temperature in the CoRoT bandpass calculated this way and including the uncertainties on the T_{eff} resulted in $T_{p,CoRoT}$ = 1910^{+90}_{-100} K. If we further assume that $F_{p,internal}$ = 0 and that the planet is in thermal equilibrium[1], this temperature favors high values of the re-distribution factor $f = 0.60 \pm 0.14$ that are greater than the maximum expected for no re-distribution from the day to the night sides ($f = 0.5$). This may be explained by (i) departures from a blackbody planetary emission; (ii) a non-zero albedo; or (iii) emission of significant internal energy from the planet. We defer the first possibility to future studies of radiative transfer in this planet.

Assuming blackbody radiation and negligible $F_{p,internal}$, Fig. 6 shows that likely values of the albedo (corresponding to f between 0.25 and 0.5) are A_g = 0.06 ± 0.06, which confirms the very low reflection of the planet obtained theoretically (e.g. Marley et al. 1999; Sudarsky et al. 2000; Seager et al. 2000; Hood et al. 2008), and observationally: upper limits for the albedos of exoplanets in similar conditions as CoRoT-2b have been reported by Charbonneau et al. (1999, A_g < 0.3 for τ Bootis b), Leight et al. (2003a,b, A_g < 0.39 for τ Bootis b, A_g < 0.12 for HD 75 289), by Rowe et al. (2008) on HD 209458b (a 3-σ upper limit of 0.17). Finally, CoRoT-1b was found to be such that A_g < 0.20 using CoRoT's red channel of the light curve (Snellen et al. 2009), and independently by Alonso et al. (2009b) using the white channel.

To distinguish among the different components of the observed planetary flux, we would need chromatic information. The CoRoT data are delivered in three band-passes, but we could not reach the level of precision needed to detect the secondary in these data. We attribute this to the difficulty of achieving a good correction of the jitter in the satellite's pointing.

As a concluding remark, the depth of the secondary eclipse of CoRoT-2b is roughly the same as a transit of a $1R_\oplus$ planet in front of a solar radius star. The significance of the detection of
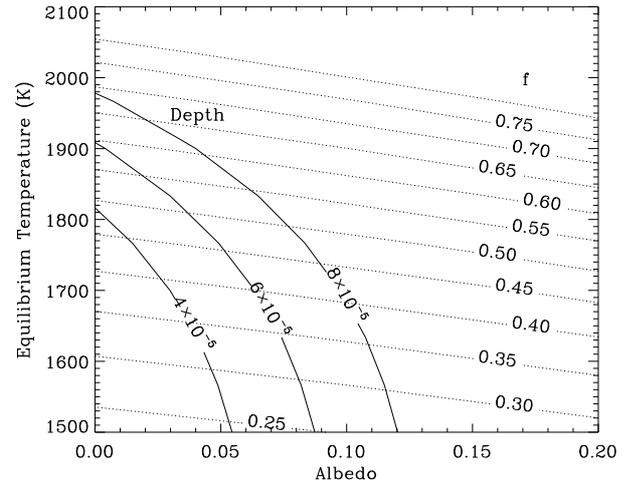
Fig. 6. The equilibrium temperature of CoRoT-2b as a function of the albedo matching the observed secondary eclipse depth. The zero-albedo equilibrium temperature is about 1910 K. The dotted lines plot the re-distribution factors f. Realistic re-distribution factors require the contribution of some reflected light (non-zero albedo) or the presence of an additional source of energy in the planet (assumed zero in this plot).

the secondary eclipse thus emphasizes the excellent capabilities of the CoRoT mission at detecting planets with radii of only a few $R_\oplus$.

References

Alonso, R., Auvergne, M., Baglin, A., et al. 2008, A&A, 482, L21
Alonso, R., Aigrain, S., Pont, F., Mazeh, T., & The CoRoT Exoplanet Science Team 2009a, IAU Symp., 253, 91
Alonso, R., et al. 2009b, A&A, submitted
Auvergne, M., et al. 2009, A&A, accepted [arXiv:0901.2206v1]
Baglin, A., Auvergne, M., Boisnard, L., et al. 2006, 36th COSPAR Scientific Assembly, 36, 3749
Bouchy, F., Queloz, D., Deleuil, M., et al. 2008, A&A, 482, L25
Burrows, A., Hubeny, I., Budaj, J., Knutson, H. A., & Charbonneau, D. 2007, ApJ, 668, L171
Charbonneau, D., Noyes, R. W., Korzennik, S. G., et al. 1999, ApJ, 522, L145
Charbonneau, D., Allen, L. E., Megeath, S. T., et al. 2005, ApJ, 626, 523
Deming, D., Seager, S., Richardson, L. J., & Harrington, J. 2005, Nature, 434, 740
Fortney, J. J., Lodders, K., Marley, M. S., & Freedman, R. S. 2008, ApJ, 678, 1419
Hood, B., Wood, K., Seager, S., & Collier Cameron, A. 2008, MNRAS, 389, 257
Jackson, B., Barnes, R., & Greenberg, R. 2009, ApJ, in press
Karkoschka, E. 1994, Icarus, 111, 174
Knutson, H. A., Charbonneau, D., Allen, L. E., et al. 2007, Nature, 447, 183
Knutson, H. A., Charbonneau, D., Allen, L. E., Burrows, A., & Megeath, S. T. 2008, ApJ, 673, 526
Knutson, H. A., Charbonneau, D., Burrows, A., O'Donovan, F. T., & Mandushev, G. 2009, ApJ, 691, 866
Lanza, A. F., Pagano, I., Leto, G., et al. 2009, A&A, 493, 193
Leigh, C., Cameron, A. C., Horne, K., Penny, A., & James, D. 2003a, MNRAS, 344, 1271
Leigh, C., Collier Cameron, A., Udry, S., et al. 2003b, MNRAS, 346, L16
Lenz, P., & Breger, M. 2005, Commun. Asteroseismol., 146, 53
Marley, M. S., Gelino, C., Stephens, D., et al. 1999, ApJ, 513, 879
Pickles, A. J. 1998, PASP, 110, 863
Pont, F. 2009, MNRAS, in press
Rowe, J. F., Matthews, J. M., Seager, S., et al. 2008, ApJ, 689, 1345
Seager, S., Whitney, B. A., & Sasselov, D. D. 2000, ApJ, 540, 504
Snellen, I. A. G., de Mooij, E. J. W., & Albrecht, S. 2009, Nature, 459, 543
Sudarsky, D., Burrows, A., & Pinto, P. 2000, ApJ, 538, 885
Valio, A., et al. 2009, A&A, submitted

---

[1] $T_{eq} = T_\star (R_\star/a)^{1/2} [f(1-A)]^{1/4}$.